Scope
Volume 13 Number 4 December 2023

Maximum Power Point Tracking Improvement Using Incorporated Linear Quadratic Regulator and Model Reference Adaptive Control Scheme

Idaresit I. Abraham[1], Christian C. Mbaocha[2], Samuel O. Okozi[3], Mfonobong E. Benson[4]

[1,2,3&4] Electrical and Electronic Engineering, Federal University of Technology, Owerri, Imo State

Abstract:
This paper presents maximum power point tracking improvement using the incorporated linear quadratic regulator (LQR) and model reference adaptive control scheme (MRAC). Solar photovoltaic energy system is one of the renewable energy applications which operates by tracking energy from the sun and converting it into useful electrical energy However, harnessing the generated energy has been the major concern of the engineers hence the necessity for an optimal control technique aimed at obtaining efficient control of the generated power hence the need for an efficient maximum power point tracking (MPPT) mechanism. This paper therefore presents MPPT improvement using incorporated linear quadratic regulator and model reference adaptive control (LQR-MRAC) technique. By system implementation on MATLAB/Simulink environment, the simulation results show an average tracking efficiency of 94.45%, a rise time of 0.7s which implies its convergence speed and the control scheme is capable of operating even at higher adaptation gains in the range $\mathbf{0.5 < \Gamma < 900}$ with minimal error. From the analysis, a duty cycle of 0.6 was also observed hence implying that the active time of the LQR-MRAC-based MPPT device would be 60% of the total operating period.

Keywords: Adaptive control scheme, Improvement, Linear quadratic regulator, Maximum power point, Model reference, Solar photovoltaic energy, Tracking

I. INTRODUCTION

Solar energy is one of the most important renewable energysources. To harness this energy to the fullest, there is need to build a photovoltaic (PV) system capable of tracking maximum power hence the need for maximum power point tracking (MPPT) device. PV system is divided into two categories: Stand-alone and Grid connected PV system. For places that are away from the utility grid, stand-alone PV systems are used at those places. The maximum power extracted from the PV source depends strongly on three factors such as irradiation, load profile and temperature (Salas, Olıas, Barrado&Lazaro, 2006).

Due to its characteristics such as little maintenance, low cost and non-moving part which makes it noiseless, the PV power system is becoming increasingly important as the most available renewable source of energy. Nevertheless, irradiation and temperature in its operation brings about the nonlinear characteristic of the amount of electric power generated hence the need to control the maximum power transferred to the load (Dolara, Faranda& Leva, 2009).

The real time experiment based on voltage reference estimator (VRE) combined with Fuzzy logic control (FLC) was proposed in the previous research. The idea was to apply Fuzzy Logic approach for maximum power point tracking implemented in a real time PV system. The limitation is that Fuzzy rules are predefined based on PV specifications and there is slowness in power correction. (Napole, Derbeli&Barambones, 2021).

Another research employed MPPT Full Bridge Converter Using Fuzzy Type-2 on DC Nano Grid System and was implemented on MATLAB/Simulink software using two models. An improved efficiency was observed in Fuzzy Type-2. In model 1, Fuzzy Type-2 had 91.40% while Fuzzy Type-1 had 80.64%. In Model 2, Fuzzy Type-2 and Fuzzy Type-1 had 87.63% and 77.93% respectively. However, the system

implementation can be undesirably complex in this case. (Prastyawan, Efendi&Murdianto, 2021). Another researcher developed an LQR-based maximum power point tracking method for standalone photovoltaic system with an experimental validation. LQR method showed an improved performance when compared with that of the conventional perturbation and observation (P&O) method. The tracking speed were recorded as 0.04s and 0.165s for LQR and P&O respectively while tracking efficiency for LQR and P&O were 96.93% and 91.83% respectively but the LQR method lacks adaptive mechanism. (Anbarasi, &Kanthalakshmi, S. (2016).

A model reference adaptive control was also developed for maximum power point tracking in PV systems. The paper adopted a two-level control algorithm which are: ripple correlation control (RCC) and model reference adaptive control (MRAC) using Lyapunov approach. An improved performance was achieved with shorter time constants and overall system stability but it was discovered that high gain can cause instability. (Vyshnavi& Subramanian, 2015).Also, maximum power point tracking method using model reference adaptive control was also carried out by different researchers. In their work, a two-level control consisting of ripple correlation control (RCC) and the model reference adaptive control (MRAC) was used. The implication of the results obtained was that the proposed control algorithm enables the system to converge to the maximum power point in milliseconds but the problem was that a large magnitude of control gain may lead to oscillations at the operating point. (Khanna, et. al., 2014).

The design and implementation of an LQR-based maximum power point tracker for solar photo-voltaic system, with real time experiment, simulation and validation showed a better efficiency in LQR than others. The range of efficiency for LQR was 90.87 – 94.78% as compared to P&O with efficiency 77.60 – 79.39% and Fuzzy Logic with 85.63 – 88.88%. This method only operated on fixed gain hence parameter tuning was essential.(Karanjkar, Chatterji&Kumar, 2014).

This paper therefore presents the MPPT improvement using incorporated linear quadratic regulator and model reference adaptive control (LQR-MRAC). To achieve this aim, consideration was given to the design of the system. Therefore, the solar PV system which was to be controlled was first identified. Upon the completion of the design phase, LQR method was used to control the system. With the LQR-controlled system, an MRAC technique was employed to control the system hence the control performance measured and validated by using the existing methods such as Perturbation and Observation (P&O), Fuzzy logic, LQR and MRAC as proposed by other researchers. Such performance characteristics considered that were critical to studying the system behaviour were rise time, efficiency, duty cycle and adaptation gains.

II. MATERIALS AND METHODS

A. *System description and validation*

Figure 1 shows the block diagram of a standalone photovoltaic (PV) system. The PV system consists of PV module, power converter, MPPT controller to track maximum power, and a load. The controller has an inbuilt algorithm that ensures the extraction of maximum power from PV module at any environmental conditions. This work is focused on tracking the maximum power through the application of a two-step control algorithm consisting of LQR. The use of DC-DC converter enables the source and load impedances to be matched hence maximum power is allowed to be transferred from source to load.

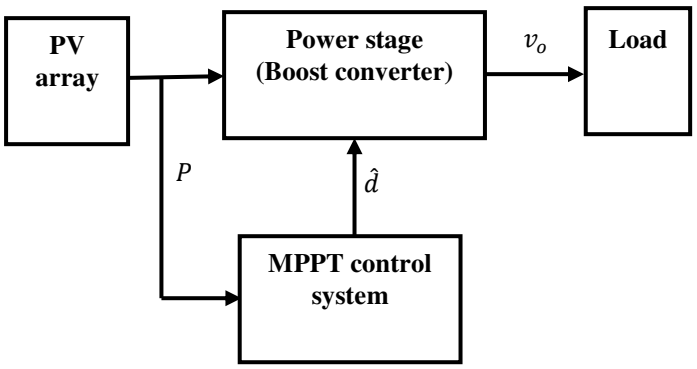

FIGURE I: BLOCK DIAGRAM OF PV SYSTEM ILLUSTRATING THE POWER SYSTEM, MPPT CONTROLLER AND LOAD

To design the system, relevant data needed for the work were extracted from Mitsubishi electric photovoltaic module specification sheet (Model: $PV-MLU255HC$, with power rating of $255W$) found online at www.studylib.net. To validate the data in the manufacturer's specification thereby making sure that the data were correct, MATLAB/Simulink was used to simulate the module using the mathematical equations (Mboumboue&Njomo, 2013;Tsai, Tu &Su, 2008;Kachhiya, Lokhande& Patel, 2011). of the photovoltaic module as in Equation (1) to Equation (4).

The photocurrent,

$$I_L = I_{sc} + K_i(T_a - T_r) \cdot \frac{\lambda}{1000} \quad (1)$$

The saturation current,

$$I_o = I_{rs}\left(\frac{T_a}{T_r}\right)^3 e^{\left[\frac{qE_{g0}}{nk}\left(\frac{1}{T_r}-\frac{1}{T_a}\right)\right]} \quad (2)$$

The reverse saturation current,

$$I_{rs} = \frac{I_{sc}}{e^{\left(\frac{qV_{oc}}{N_s k n T_a}\right)} - 1} \quad (3)$$

The PV current,

$$I_{PV} = N_p I_{ph} - N_p I_o \left\{ e^{\left[\frac{q(V_{PV}+I_{PV}R_s)}{N_s k n T_a}\right]} - 1 \right\} - \frac{V_{PV} + I_{PV}R_s}{R_p} \quad (4)$$

Where: T_r = module temperature (Kelvin), T_a = ambient temperature (Kelvin), I_{sc} = Short-circuit current,
$\lambda = Solar\ irradiance\ (W/m^2), V_{oc}$ =Open-circuit voltage,
q = charge of an electron$(1.622 \times 10^{-19} Coulumbs)$,
n = diode ideality factor $(1 < n < 2)$,
E_{g0} = bandgap energy of semiconductor $(1.1eV)$,
k = Boltzmann's constant $(1.3807 \times 10^{-23} Joules/Kelvin)$,
N_s = number of series cells (36),
N_p =number of shunt cells (1).

The Simulink models created from the module equations are shown in Figure II and Figure III, while Figure IV illustrates the P-V and I-V characteristic curves of the module obtained from the Simulink model after simulations at Standard Test Conditions (STC) of $1000W/m^2$ solar irradiance and a temperature of $25°C$. The curves therefore validate the data in Mitsubishi specification sheet. Hence the data is reliable for this research analysis.

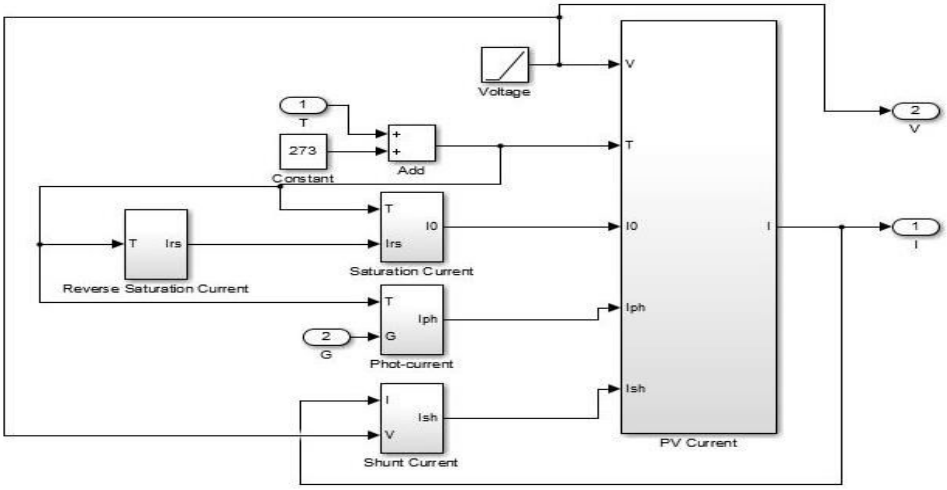

FIGURE II: SUBSYSTEMS INTERCONNECTIONS OFSIMULINK MODEL FOR THEPV MODULE

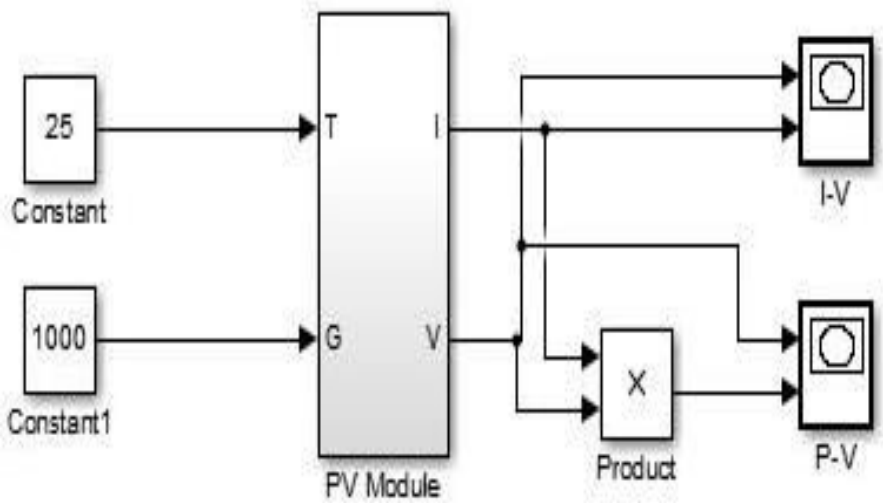

FIGURE III: SIMPLIFIED MODEL OF THE SIMULINK MODELFOR MEASUREMENT AT STC

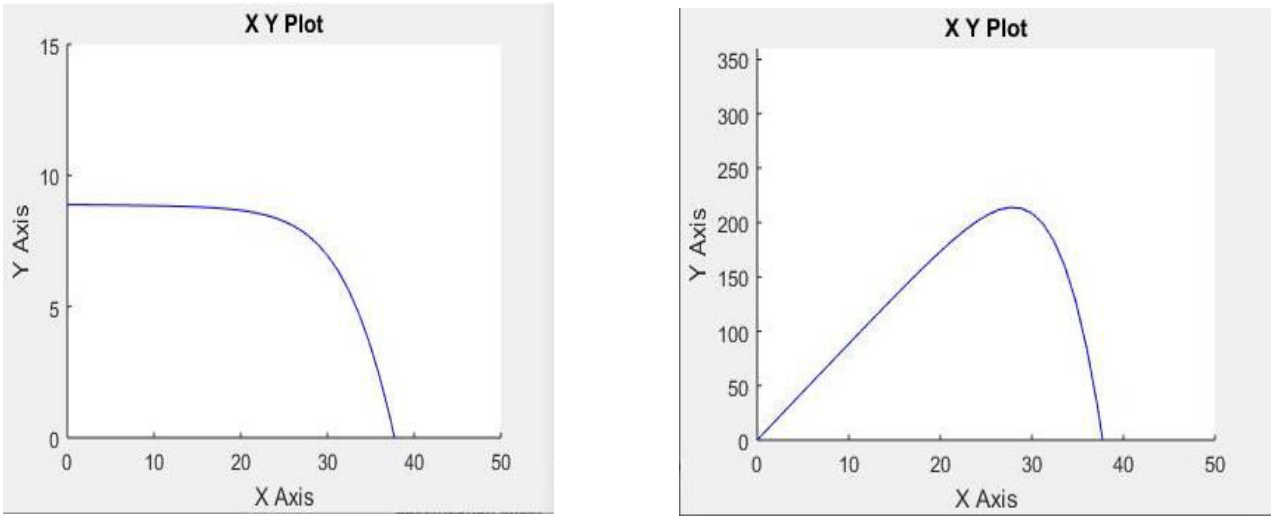

FIGURE IV: I-V AND P-V CURVES AT STC (IDARESIT ET. AL., 2023)

B. Methods

1) System design

The system (plant) to be controlled was designed by using a boost converter as shown in Figure V.

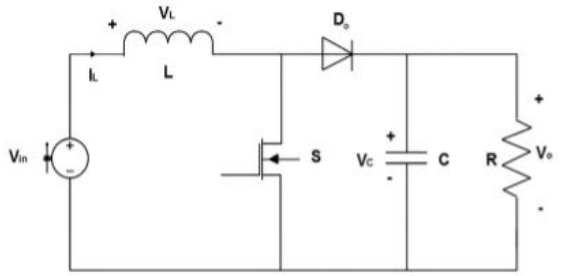

FIGURE V: GENERAL CONFIGURATION OF A BOOST CONVERTER

The converter was modelled by utilizing two switch mode – the on-state and the off-state. The state variables chosen were capacitor voltage $v_c = v_o$and inductor current i_L, and the expressions during turn on and turn off processes are written as

Case 1: *ON-MODE* $(0 \leq t < DT)$

$$L\frac{di_L}{dt} = v_{in} (5a)$$

$$C\frac{dv_o}{dt} = -\frac{v_o}{R_L} (5b)$$

Case 2: *OFF-MODE* $(DT \leq t < T)$

$$L\frac{di_L}{dt} = v_{in} - v_o (6a)$$

$$C\frac{dv_o}{dt} = i_L - \frac{v_o}{R_L} (6b)$$

Linking Equations (5a)with (6a), and equations (5b) with (6b) yields equations (7a) and (7b) respectively.

$$L\frac{di_L}{dt} = Dv_{in} + (1-D)(v_{in} - v_o) (7a)$$

$$C\frac{dv_o}{dt} = -D\frac{v_o}{R_L} + (1-D)(i_L - \frac{v_o}{R_L}) \quad (7b)$$

The small signal modelling of the system was done by setting $i_L = (I_L + \hat{\imath}_L), v_{in} = (V_{in} + \hat{v}_{in}), v_o = (V_o + \hat{v}_o)$ and$D = (d + \hat{d})$ in equation (7), to give the linearized state model of the system as in (8).

$$L\frac{d\hat{\imath}_L}{dt} = \hat{v}_{in} - (1-d)\hat{v}_o + V_o\hat{d} \quad (8a)$$

$$C\frac{d\hat{v}_o}{dt} = (1-d)\hat{\imath}_L - \frac{\hat{v}_o}{R_L} - \hat{\imath}_L\hat{d} \quad (8b)$$

By letting $\hat{\imath}_L = x_1, \hat{v}_o = x_2$, equation (8) was represented in state space formas in equation (9).

$$\begin{bmatrix}\dot{x}_1\\ \dot{x}_2\end{bmatrix} = \begin{bmatrix}0 & -\frac{1}{L}(1-d)\\ \frac{1}{C}(1-d) & -\frac{1}{CR_L}\end{bmatrix}\begin{bmatrix}x_1\\ x_2\end{bmatrix} + \begin{bmatrix}\frac{V_o}{L} & \frac{1}{L}\\ -\frac{I_L}{C} & 0\end{bmatrix}\begin{bmatrix}\hat{d}\\ \hat{v}_{in}\end{bmatrix} (9a)$$

$$y = x_2$$
$$= [0 \quad 1]\begin{bmatrix}x_1\\ x_2\end{bmatrix} (9b)$$

2) System specifications

The specifications used in the design of the boost converter were summarized as in Table I.

TABLE I (Idaresit et. al., 2023)
SUMMARY OF THE BOOST CONVERTER DESIGN SPECIFICATION

Description of component	Rating
Input voltage (V_{in})	$31.2V$
Output capacitance (C)	$5.0mF$
Load resistance (R_L)	25.0Ω
Inductance (L)	$0.1mH$
Nominal duty ratio (D)	0.6
Switching frequency	$20kHz$

With the system of the form, $\dot{x} = Ax + Bu$ as in equation (9), the state space and output equations were respectively obtained as in equation (10) by inputting the values presented in Table I.

$$\begin{bmatrix}\dot{x}_1\\ \dot{x}_2\end{bmatrix} = \begin{bmatrix}0 & -4000\\ 80 & -8\end{bmatrix}\begin{bmatrix}x_1\\ x_2\end{bmatrix} + \begin{bmatrix}800000 & 10000\\ -1560 & 0\end{bmatrix}\begin{bmatrix}\hat{d}\\ \hat{v}_{in}\end{bmatrix} \quad (10a)$$

$$y = x_2 = [0 \quad 1]\begin{bmatrix}x_1\\ x_2\end{bmatrix} \quad (10b)$$

Where the constants, $A = \begin{bmatrix}0 & -4\times10^3\\ 80 & -8\end{bmatrix}$, $B = \begin{bmatrix}10\times10^3\\ 0\end{bmatrix}$, $C = [0 \quad 1]$ and $D = 0$

3) LQR Control system design

The following phase of the work after obtaining the system equation was the design of the control mechanism to drive the system to the required state. The first control method employed was LQR and then the result was used as a plant, which was later controlled by MRAC. LQR controller ensures that optimal power is delivered to the load by maintaining a fixed gain. The optimal control problem is defined by finding an optimal control u for the system given by

$$\dot{x}(t) = Ax(t) + Bu(t) \quad (11)$$

So as to minimize or maximize the required performance index J defined by,

$$J = \int_0^t (x^T Q x + u^T R u)dt \quad (12)$$

where Q and R are the weighting matrices that should be chosen in order to give the minimum value of the performance index (J). To achieve the required objectives, the followingthree important steps wereconsidered:

Selecting the state and control penalty matrices, *Q* and *R* respectively: The Q matrix was selected by varying the Q_{22}component while all other component values were set to zero while R was kept constant. The corresponding step responses for each value of Q_{22} were plotted as shown in Figure 5.By varying the values of $\boldsymbol{Q_{22}}$ the performance of the system was studied from the plotted graph and recorded as shown in Table II. The value that yielded the minimal error

between the output signal and the reference was selected though settling time and overshoot were not also neglected in the selection criteria. Having adopted such a procedure in the work, Q_{22} was found to be 0.8, which has the settling time 0.0062s and overshoot of 15%. Therefore, the state penalty matrix and the control penalty matrix were recorded as

$$Q = \begin{bmatrix}0 & 0\\ 0 & 0.8\end{bmatrix} \text{ and } R = 1 \quad (13)$$

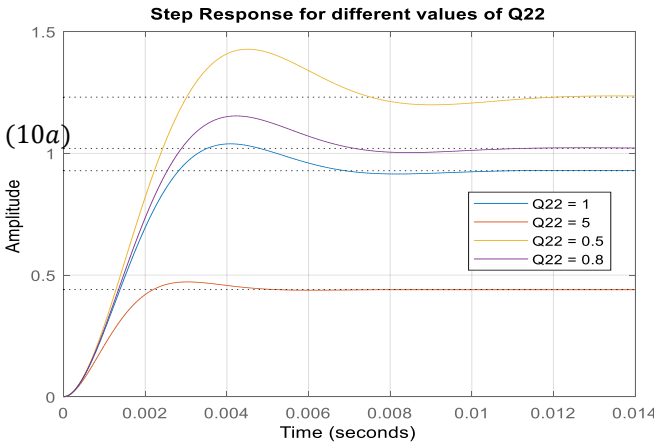

FIGURE VI: TIME RESPONSE FOR VARYING VALUES OF $\boldsymbol{Q_{22}}$

Solving the Algebraic Riccatti equation: The Algebraic Riccati equation (14a), was solved to obtain the $\boldsymbol{P}$matrix by applying a MATLAB code$[K, P, E] = lqr(A, B, Q, R)$.

$$\dot{P} = PA + A^T P + Q - PBR^{-1}B^T P = 0 \quad (14a)$$

The solution yields,

$$P = \begin{bmatrix}0.0000 & 0.0001\\ 0.0001 & 0.0012\end{bmatrix} \quad (14b)$$

Obtaining the feedback gain:The feedback gain $\boldsymbol{K}$ defined by equation (15) as well as the eigenvalues$E$were also obtained simultaneously from the MATLAB code above.

$$K = R^{-1}B^T P$$

$$K = [0.0955 \quad 0.5702] \quad (15b)$$

$$E = -481.6 \pm j742.9 \quad (15c)$$

Hence, the optimal controller $u(t)$ obtained as,

$$u(t) = R^{-1}B^T P\, x(t) = -Kx(t) \quad (16a)$$

$$u(t) = -[0.0955 \quad 0.5702]\begin{bmatrix}x_1\\ x_2\end{bmatrix}$$

Therefore, the corresponding closed-loop system equation was computed as,

$$\begin{bmatrix}\dot{x}_1\\ \dot{x}_2\end{bmatrix} = \begin{bmatrix}-955.2 & -9702.4\\ 80 & -8\end{bmatrix}\begin{bmatrix}x_1\\ x_2\end{bmatrix} + \begin{bmatrix}10000\\ 0\end{bmatrix}u \quad (17a)$$

$$y = x_2 = [0 \quad 1]\begin{bmatrix} x_1 \\ x_2 \end{bmatrix} \quad (17b)$$

$Where: A_{cl} = A - BK = \begin{bmatrix} -955.2 & -9702.4 \\ 80 & -8 \end{bmatrix}$; $B_{cl} = \begin{bmatrix} 10000 \\ 0 \end{bmatrix}$; $C_{cl} = [0 \quad 1]$ and $D_{cl} = 0$

Hence, by using $G(s) = C(sI - A)^{-1}B_1 + D$ the state space equation was transformed to a transfer function thus:

$$G(s) = \frac{800000}{s^2 + 963.2s + 768550.4} \quad (18)$$

4) MRAC system design

The function of the adaptive control mechanism is to ensure that the controller parameters are adjusted with respect to changes in environmental conditions so as to generate the suitable control law capable of driving the plant to meet the required power demand. The system compares the plant's output with the output of the reference model and generates an error signal which is used by adaptation mechanism to update the controller parameters for effective power optimization. The block diagram of the proposed control architecture is as shown in figure VII.

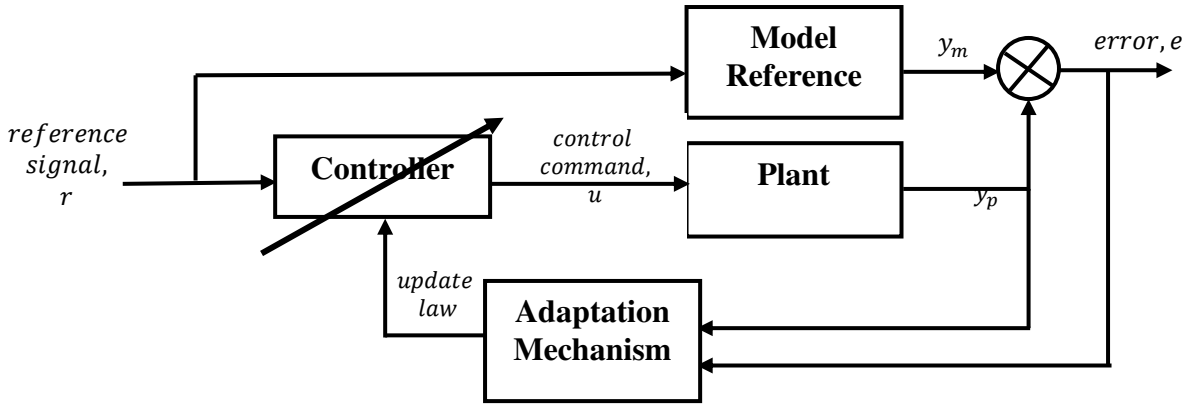

FIGURE VII: GENERIC BLOCK DIAGRAM OF MRAC CONTROL SYSTEM

To realize the objective of this work, four steps were taken into consideration to derive the adaptation law for controller parameters in MRAC:

Choosing the controller structure: The control law was chosen as,

$$u = r\theta_1 - y_p\theta_2 \quad (19)$$

Finding state-space expressions for the controlled plant and the reference model: Given the process dynamics and reference model systems,

$$Y_p(s) = \frac{k_p}{s^2 + a_p s + b_p}U(s) \quad (20a)$$

$$Y_m(s) = \frac{k_m}{s^2 + a_m s + b_m}R(s) \quad (20b)$$

Rewriting the system as a first order state-space form, Equation (20) yields,

$$\dot{y}_p = -A_p y_p + B_p u \quad (21a)$$

$$\dot{y}_m = -A_m y_m + B_m r \quad (21b)$$

Substituting Equation (19) in (21) and simplifying, we have

$$\dot{y}_p = -(A_p + B_p\theta_2)y_p + B_p\theta_1 r \quad (22)$$

This implies that for the process dynamics to match the reference model then,

$$\theta_1 = \frac{B_m}{B_p} \text{and} \theta_2 = \frac{A_m - A_p}{B_p} \quad (23)$$

Constructing error equations: Let the error $e = y_p - y_m$ so that,

$$\dot{e} = \dot{y}_p - \dot{y}_m \quad (24)$$

$$\dot{e} = -A_m(y_m - y_p) - (B_p\theta_2 + A_p - A_m)y_p + (B_p\theta_1 - B_m)r \quad (25)$$

Deriving an adaptation law for MRAC: By Lyapunov function,

$$V(e,\theta_1,\theta_2) = \frac{1}{2}\Gamma e^2 + \frac{1}{2B_p}(B_p\theta_1 - B_m)^2 + \frac{1}{2B_p}(B_p\theta_2 + A_p - A_m)^2 \quad (26)$$

$$\dot{V}(e,\theta_1,\theta_2) = \Gamma e\dot{e} + (B_p\theta_1 - B_m)\dot{\theta}_1 + (B_p\theta_2 + A_p - A_m)\dot{\theta}_2 \quad (27)$$

$$\dot{V}(e,\theta_1,\theta_2) = -\Gamma A_m e^2 + (\Gamma er + \dot{\theta}_1)(B_p\theta_1 - B_m) + (-\Gamma e y_p + \dot{\theta}_2)(B_p\theta_2 + A_p - A_m) \quad (28)$$

Therefore, the update law was obtained from Equation (28) as,

$$\dot{\theta}_1 = -\Gamma er \quad (29a)$$

$$\dot{\theta}_2 = \Gamma e y_p \quad (29b)$$

Where Γ is adaptation gain.

Reference model design

A critically damped system designed to be the reference model y_m such that the damping ratio $\xi = 1$ and$\omega_n = 481.6rad/s$, hence ${\omega_n}^2 = 231938.56rad^2/s^2$ and $2\xi\omega_n = 963.2rad/s$. The value of $k_m = 240000$ was chosen for the reference model after series of tests by simulation such that the value of $k_m \geq {w_n}^2$. The designed reference model is given by:

$$G(s) = \frac{240000}{s^2 + 963.2s + 231938.56} \quad (30)$$

From the mathematical designs above, LQR-MRAC Simulink model was obtained as shown in Figure VIII.

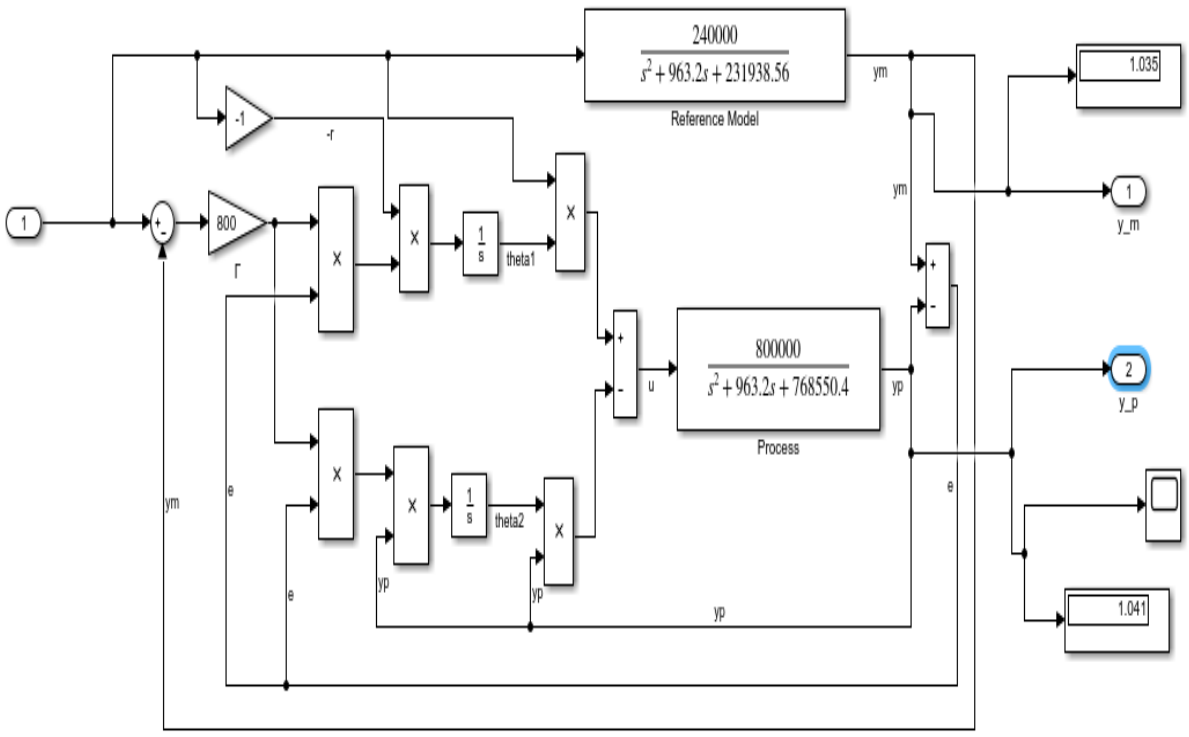

FIGURE VIII: LQR-MRAC CONTROL SIMULINK MODEL OF MRAC-ONLY CONTROL SCHEME

III. RESULTS

Figures IX, X XI, XII an XIII show the performance of the system for different adaptation gain values. The figures illustrate the behaviour of the system hence shows the measured output signal, output error, control signal, and parameter estimations (for θ_1 and θ_2) respectively.

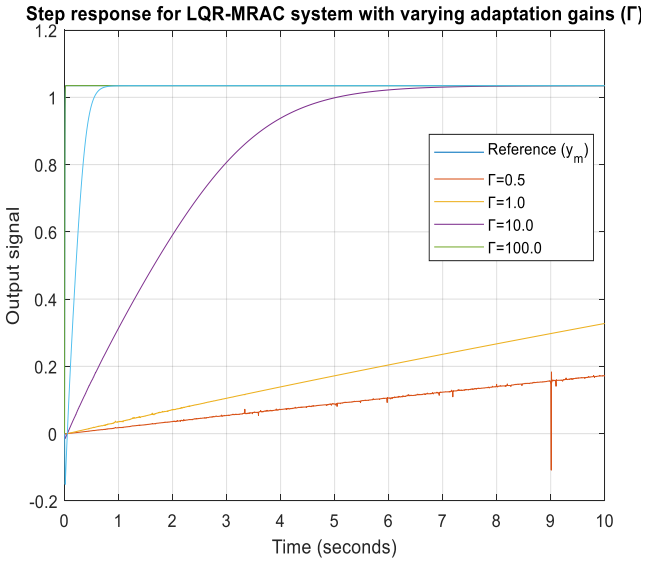

FIGURE IX: TIME RESPONSE CURVE ILLUSTRATING THE OUTPUT SIGNALFOR DIFFERENT GAIN VALUES

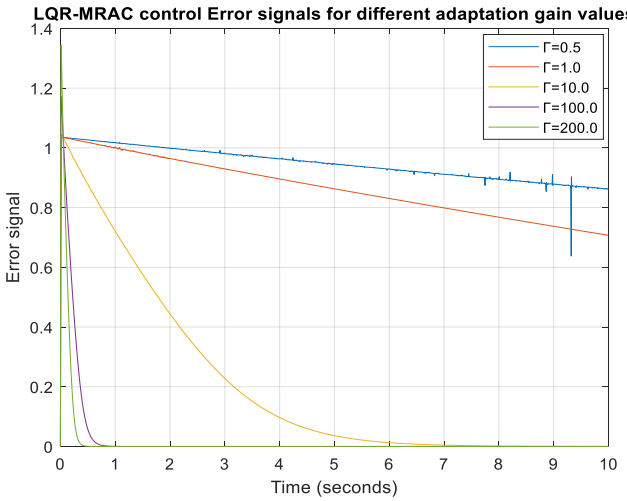

FIGURE X: TIME RESPONSE CURVE ILLUSTRATING THE OUTPUT ERROR FOR DIFFERENT GAIN VALUES

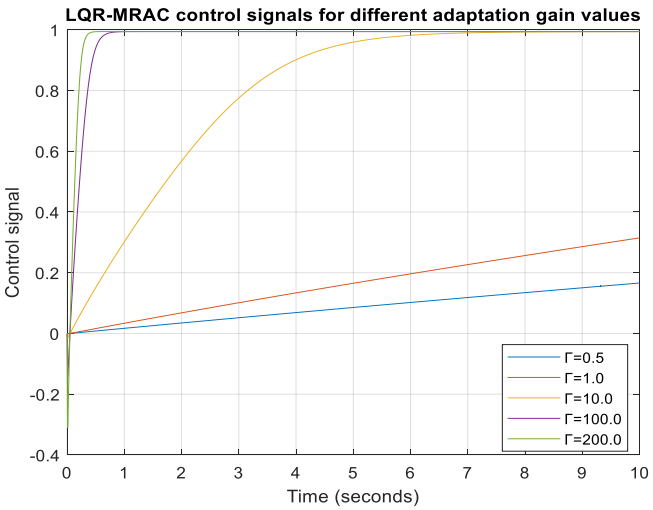

FIGURE XI: TIME RESPONSE CURVE ILLUSTRATING THE CONTROL SIGNAL FOR DIFFERENT GAIN VALUES

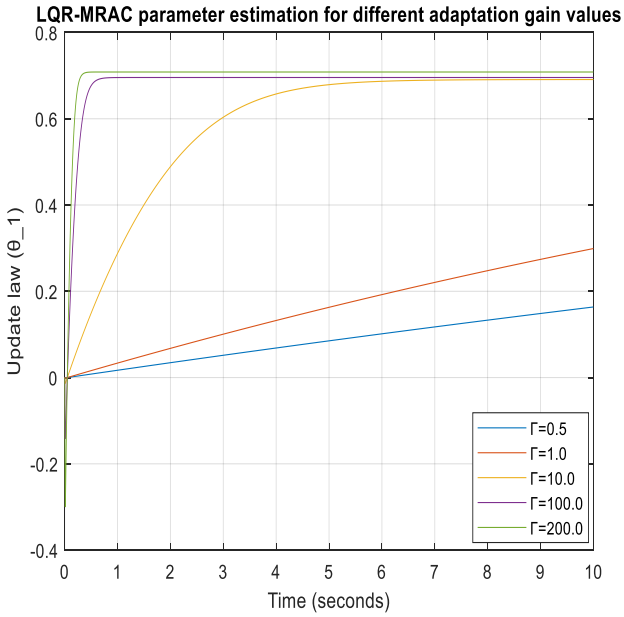

FIGURE XII: PARAMETER ESTIMATION ILLUSTRATING UPDATE LAW $[\theta_1]$ FOR DIFFERENT GAIN VALUES

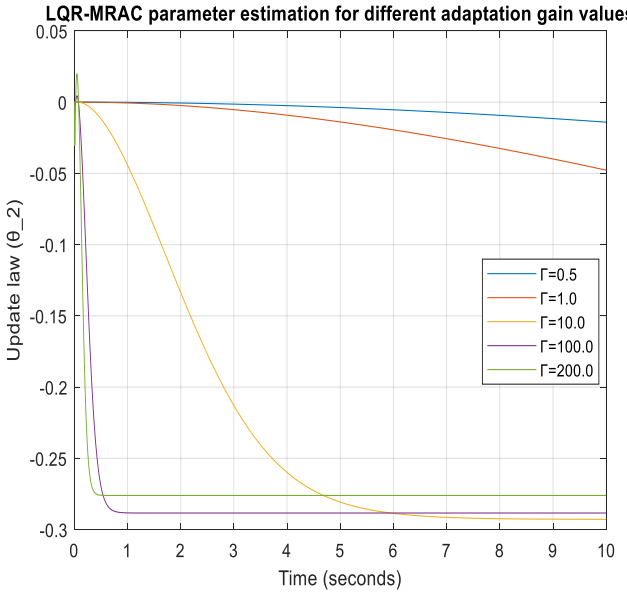

FIGURE XIII: PARAMETER ESTIMATION ILLUSTRATING UPDATE LAW $[\theta_2]$FOR DIFFERENT GAIN VALUES

Table II shows the summary of the performance for the system as per different gain values while Table III shows the summary of the performance result measured from the plotted graph. Such parameters considered were efficiency, duty cycle, rise time and adaptation gain values.

TABLE II

SYSTEM PERFORMANCE AS PER DIFFERENT ADAPTATION GAINS

AdaptationGain	θ_1	θ_2	Rise time (secs.)	Steady state
0.005	0.001788	-0.000001674	2.220	0.001696
0.05	0.01773	-0.0001638	2.743	0.01838
0.1	0.03515	-0.0006431	2.289	0.03646
0.5	0.1636	-0.01404	5.377	0.1726
1	0.2991	-0.04773	0.0019	0.3276
2	0.495	-0.1373	6.143	0.6011
3	0.6061	-0.2152	7.719	0.813
4	0.6583	-0.2609	7.260	0.9407
5	0.6792	-0.2811	6.534	0.9995
10	0.691	-0.2928	3.537	1.035
25	0.6914	-0.2925	1.409	1.035
50	0.6924	-0.2915	0.707	1.035
100	0.6957	-0.2884	0.354	1.035
200	0.7084	-0.2761	0.178	1.035
400	0.7728	-0.2138	0.098	1.035
500	0.8417	-0.1472	0.1004	1.035
800	1.351	-0.3446	0.000881	1.035
900	0.9401	-0.05219	0.000156	1.035
950	199.8	194.9	0.000038	0.7267

TABLE III

SUMMARY OF THE MEASURED PARAMETERS

Parameter	Values
Rise time	709.300ms
Tracking efficiency	94.45%
Duty cycle	0.632
Adaptation gain values	$0.5 < \Gamma < 900$

IV. DISCUSSION

To validate the result, the performance of incorporated LQR-MRAC obtained upon simulation were compared with the performance of the existing control techniques such as LQR, MRAC, P&O, etc. carried out by other researchers.

The results showed an improved tracking efficiency for the incorporated LQR-MRAC system, which has an efficiency of 94.45% compared to an efficiency of 91.83% for P&O as proposed by (Anbarasi&Kanthalakshmi, 2016).

The control method also showed an improved efficiency over Fuzzy Logic with an average efficiency of 87.26% as proposed by (Karanjkar, Chatterji& Kumar, 2014)in their work. Though (Anbarasi&Kanthalakshmi, 2016) recorded an efficiency of 96.63% for LQR, which is closed to the value obtained in this present work, it is worthy to note that LQR control lacks the adaptation features required to compensate for environmental changes since the system only utilizes the fixed optimal gain designed originally for the system hence, LQR-MRAC would operate under varying conditions of the environment because of the integration of the adjustable mechanism in the system.

In another case, it should be noted that incorporated LQR-MRAC also showed an improved performance feature in terms of its nature of operation when compared with the MRAC-only scheme. (Vyshnavi& Subramanian, 2015)observed that though MRAC achieved an improved performance with shorter time constants but it was discovered that high gain can cause instability and in RCC-MRAC two-level control, (Khanna et. al., 2014)stated in their work that the control algorithm enables the system to converge to the maximum power point in milliseconds but the problem was that a large magnitude of control gain might lead to oscillations at the operating point. However, it is obvious that the LQR-MRAC-based system could operate accurately even at higher gain values compared to MRAC-only and RCC-MRAC techniques proposed previously.

Further analysis showed that the rise time for the LQR-MRAC-based control was about 0.7s which is higher than that of the LQR and P&O, with the rise time of 0.04s and 0.165s

respectively proposed by (Anbarasi&Kanthalakshmi, 2016), which implies that LQR-MRAC-based control is slower in convergence speed. Moreover, LQR-MRAC yields the duty cycle of 0.6 hence implying that the time at which the system could be active is 60% of the total operating period.

.

V. CONCLUSIONS

The need for optimal control in solar photovoltaic energy systems arises as a result of the non-linear characteristic of the P-V characteristic curve, which is dependent on the environmental conditions such as irradiation and temperature, and so on. Such conditions therefore bring about unstable output power such that the power transferred to the load is not maximum. For this reason, different control strategies have been adopted by researchers to ensure that optimal output power is achieved. The idea of this work was therefore to investigate the behaviour of the solar PV system as it was being controlled by incorporated LQR-MRAC method. The results showed that this control strategy accepts higher adaptation gains which may be in the range $0.5 < \Gamma < 900$ contrary to MRAC-only, whose gains must be kept small to avoid oscillations. Since LQR only operated at a fixed optimal gain of which it was originally designed, it was obvious that LQR system would not function optimally if deviation from the original design occurred, hence LQR-MRAC-based system became a better alternative method since it would still operate at varying gains. Also, the efficiency (94.45%) of the control method was better compared to MRAC-only, Fuzzy logic, P&O. However, it was observed upon simulation that the limitation of LQR-MRAC was slowness in convergence speed compared to P&O, LQR, etc. as its rise time was found to be 0.7s. Finally, LQR-MRAC was found to have a duty cycle of 0.6, which implies the active time factor of the system. For future research direction, the system could be improved by considering the alternative to improve the convergence speed.

VI. REFERENCES

Salas, V., Olıas, E., Barrado, A., Lazaro, A. (2006). "Review of the maximum power point tracking algorithms for stand-alone photovoltaic systems." ELSEVIER Solar Energy Materials & Solar Cells, Vol. 90, pp. 1555–1578.

Dolara, A., Faranda, R. and Leva, S. (2009). "Energy comparison of seven MPPT techniques for PV systems." *Journal of Electromagnetic Analysis and Applications*. Vol. 1, No. 3, pp.152–162.

Napole, C., Derbeli, M. and Barambones, O. (2021). Fuzzy Logic Approach for Maximum Power Point Tracking Implemented in a Real Time Photovoltaic System. *Journal of Applied Sciences.* Vol. 11, No. 5927 pp. 1 – 18..

Prastyawan, A., Efendi, M. and Murdianto, F. (2021). "MPPT Full Bridge Converter Using Fuzzy Type-2 on DC Nano Grid System." *Journal on Advanced Research in Electrical Engineering.* Vol. 5, No. 2, pp. 120 – 127.

Anbarasi, M. and Kanthalakshmi, S. (2016). "Linear quadratic optimal control of solar photovoltaic system: An experimental validation." *Journal of Renewable and Sustainable Energy.* Vol. 8..

Vyshnavi, N. and Subramanian, K. (2015). "Model reference adaptive control for maximum power point tracking in PV systems." IJARIIE - ISSN(O) – 2395-4396. Vol-1 Issue-5, pp. 556 – 568. www.ijariie.com.

Khanna, R., Zhang, Q., Stanchina, W. E., Reed, G. F. and Mao, Z. (2014). "Maximum Power Point Tracking Using Model Reference Adaptive Control." IEEE Transactions on Power Electronics. Vol. 29, No. 3, pp. 1490 – 1499.

Karanjkar, D. S., Chatterji, S. and Kumar, A. (2014). "Design and Implementation of a Linear Quadratic Regulator Based Maximum Power Point Tracker for Solar Photo-Voltaic System." *International Journal of Hybrid Information Technology*. Vol.7, No.1, pp. 167-182. ISSN: 1738-9968 IJHIT Copyright ⓒ 2014 SERSC.

Mboumboue, E. and Njomo, D. (2013). "Mathematical Modeling and Digital Simulation of PV Solar Panel using MATLAB Software." International Journal of Emerging Technology and Advanced Engineering. Vol. 3, Issue 9, pp. 24 – 32. Website: www.ijetae.com (ISSN 2250- 2459, ISO 9001:2008 Certified Journal).

Tsai, H., Tu, C. and Su, Y. (2008). "Development of Generalized Photovoltaic Model Using MATLAB/SIMULINK." Proceedings of the World Congress on Engineering and Computer Science, WCECS 2008, San Francisco USA, pp. 1-6.

Kachhiya, K., Lokhande, M. and Patel, M., (2011). "MATLAB/Simulink Model of Solar PV Module and MPPT Algorithml." National Conference on Recent Trends in Engineering & Technology. B. V. M. Engineering College, V. V. Nagar, Gujarat India, pp. 1-5, 13-14.

BIBLIOGRAPHY

Abdelsalam, A. K., Massoud, A. M., Ahmed, S. and Enjeti, P. N. (2011). "High-Performance Adaptive Perturb and Observe MPPT Technique for Photovoltaic-Based Microgrids." IEEE Transactions on Power Electronics. Vol. 26, No. 4, pp. 1010 – 1021.

Ahmed, M. E., Mousa, M. and Orabi, M. (2010). "Development of high gain and efficiency photovoltaic system using multilevel boost converter topology." International Proceedings of the 2nd International Symposium on Power Electronics for Distributed Generation Systems, Hefei, China, 16–18 June 2010; pp. 898–903.

Akihiro, O. (2005) "Design and simulation of photovoltaic water pumping system." A thesis presented to the Faculty of California Polytechnic State University, San Luis Obispo. pp. 5 – 36.

Elgendy, M. A., Zahawi, B. and Atkinson, D. J. (2012). "Assessment of perturb and observe MPPT algorithm implementation techniques for PV pumping applications." IEEE Transactions on Sustainable Energy. Vol.3, No.1, pp. 21–33.

Jain, P. and Nigam, M. J. (2013). "Design of a Model Reference Adaptive Controller Using Modified MIT Rule for a Second Order System." Advance in Electronic and Electric Engineering. ISSN 2231-1297, Vol. 3, No. 4, pp. 477-484 © Research India Publications www.ripublication.com.

Mitsubishi Photovoltaic Module specification sheet (MLU): 250-255W[online], www.studylib.net

ACKNOWLEDGEMENTS

Firstly, we express our profound gratitude to the Almighty God for His Grace towards the success of this work. Secondly, we wish to appreciate our friends, colleagues, advisors and lecturers in the Department of Electrical and Electronic Engineering, Federal University of Technology, Owerri, Nigeria for their advice, mentorship, ideas and other relevant supports. We thank Mfonobong Eleazar Benson, a colleague for his contributions and selfless assistance, during the course of this work.